

# Ab initio study of a mechanically gated molecule: From weak to strong correlation

A. Greuling<sup>1</sup>, M. Rohlfing<sup>1,\*</sup>, R. Temirov<sup>2</sup>, F.S. Tautz<sup>2</sup>, and F.B. Anders<sup>3</sup>

<sup>1</sup>Fachbereich Physik, Universität Osnabrück, BarbarasträÙe 7, 49069 Osnabrück, Germany

<sup>2</sup>Institut für Bio- and Nanosysteme, Forschungszentrum Jülich, 52425 Jülich, Germany

<sup>3</sup>Fakultät für Physik, TU Dortmund, Otto-Hahn-StraÙe 4, 44227 Dortmund, Germany

(Dated: February 20, 2018)

The electronic spectrum of a chemically contacted molecule in the junction of a scanning tunneling microscope can be modified by tip retraction. We analyze this effect by a combination of density functional, many-body perturbation and numerical renormalization group theory, taking into account both the non-locality and the dynamics of electronic correlation. Our findings, in particular the evolution from a broad quasiparticle resonance below to a narrow Kondo resonance at the Fermi energy, correspond to the experimental observations.

Both the control of the geometric structure of a molecular junction and the systematic manipulation of its electronic structure by an external parameter are of central importance for molecular electronics [1]. So far, the best control over the geometric junction structure is reached in experiments based on scanning tunnelling microscopy (STM) [2, 3], because they allow the selection of an individual molecule in a specific environment and its contacting with the STM tip at a defined position within the molecule (e.g. ref [4]). On the other hand, the most common approach to tuning the electronic structure, electrical gating, is difficult to combine with STM. However, in a recent experimental study [5] we contacted a surface-adsorbed molecule with an STM tip and peeled it off the surface by tip retraction, as shown schematically in Fig. 1. Spectroscopic data recorded during tip retraction revealed a *mechanical* gating effect, in the sense that one of the molecular orbitals responds to the structural change and shifts with respect to the Fermi level ( $E_F$ ) of the substrate, before becoming pinned at  $E_F$  (Fig. 2d).

In this letter we use this experiment, which was carried out on 3,4,9,10-perylene-tetracarboxylic-dianhydride (PTCDA) adsorbed on the Ag(111) surface, as a motivation for a theoretical study of the interplay between the geometric structure and the electronic spectrum of a molecular junction. The mechanical gating is subject to subtle details of electronic correlation, e.g. screening of the intramolecular Coulomb repulsion by the electrodes, which is not described by conventional density-functional theory (DFT). We therefore propose the following strategy: DFT addresses the atomistic details of the junction structure but does not provide reliable, well-founded spectral data. To evaluate the electronic spectrum, we combine DFT with many-body perturbation theory (MBPT) [6] for non-local correlation and with numerical renormalization-group (NRG) theory [7] for correlation dynamics beyond the mean-field level. We stress that only by combining DFT, MBPT and NRG a well-founded picture emerges, which can be systematically compared to the data presented in Ref. [5] and the (more comprehensive) experiment in Fig. 2d.

We first discuss the geometric structure of the

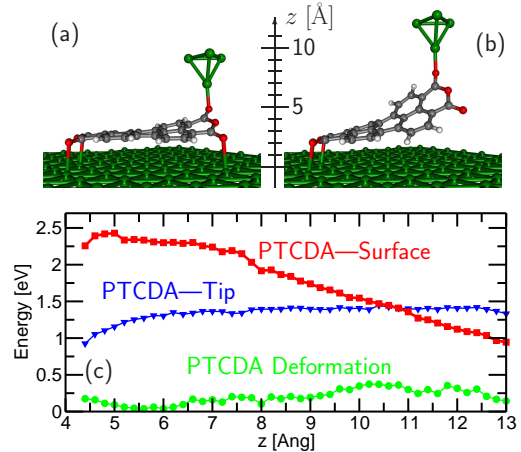


FIG. 1: DFT-LDA data of tip/PTCDA/Ag(111) junction. (a, b) Two representative configurations at tip-surface distances of  $z = 7 \text{ \AA}$  and  $z = 10 \text{ \AA}$ , respectively. For better visibility only a section of the tip and the substrate are shown. (c) Bond energies of the PTCDA-tip and PTCDA-surface bonds as a function of tip height  $z$ . At each  $z$  the molecule has been fully relaxed. The internal deformation energy of the PTCDA reflects the bending and twisting of its perylene core.

tip/PTCDA/Ag(111) junction in the framework of the local density approximation (LDA) to DFT [8]. PTCDA molecules adsorb on the Ag(111) surface in a flat-lying configuration [9–13]. Several DFT studies of the adsorption have been published (for details, see Ref. [14] and references therein). Following experiment [5], we place the tip, which in our simulation consists of ten Ag atoms in a pyramidal shape [15], above one of the carboxylic oxygen atoms and approach it to the surface. At a tip-surface distance of  $z = 6.2 \text{ \AA}$  ( $6.7 \text{ \AA}$  in experiment [5]) the oxygen atom jumps up and forms a covalent bond with the tip apex atom. The tip can then be moved up and down reversibly, forcing the oxygen atom and the attached section of the PTCDA molecule to follow, resulting in a peeling-like motion (Fig. 1a-b). Throughout the paper,  $z$  specifies the vertical distance between the tip apex atom and the uppermost surface layer.

Some representative DFT-LDA data of the structure and energetics of the junction are displayed in Fig. 1. Fig. 1 a and b shows two typical configurations. At a tip-surface distance of  $z = 7 \text{ \AA}$  only a small section of the molecule is detached from the surface, while at  $z = 10 \text{ \AA}$  about half of the molecule has lost contact with the substrate. The continuous nature of the peeling process as a function of  $z$  is reflected in the smooth behavior of the molecule-tip and molecule-surface bond energies (Fig. 1c) and in a smooth  $z$ -dependence of all intramolecular structural parameters.

The most interesting feature of the electronic structure of the junction is the PTCDA LUMO (lowest unoccupied molecular orbital), because this is the orbital for which the gating effect as a function of the external parameter  $z$  is observed [5]. In the gas phase, the LUMO is found  $\sim 2 \text{ eV}$  above the Ag(111) Fermi level (Fig. 2a). Upon adsorption, the LUMO is lowered in energy below the Ag(111) Fermi level due to the metallic polarizability of the substrate [19–21] and thus becomes partially occupied with about 1.8 electrons (counterbalanced by back-donation from other molecular states to the surface).

The partial occupation of the LUMO (which changes as a function of  $z$ ; see below) causes the high sensitivity of the LUMO spectrum to the junction structure: In experiment, for  $z$  below  $8.2 \text{ \AA}$  the LUMO approaches the Fermi energy at a steep slope of  $\sim 0.2\text{--}0.3 \text{ eV/\AA}$  and turns into a sharp resonance as soon as it reaches  $E_F$  at  $z = 8.2 \text{ \AA}$ . At  $z = 9.7 \text{ \AA}$ , the FWHM of the LUMO peak is  $14 \text{ meV}$ . We note that although a mechanical gating effect is observed already in DFT-LDA (top curves in Fig. 2b-c and open circles in Fig. 2d), there is a large discrepancy with the experimental data: The DFT-LDA LUMO reaches the Fermi level far too late (at  $12 \text{ \AA}$ ), and it does not sharpen as much as in experiment. Because of this sharpening, the experimental resonance at the Fermi level has been discussed in terms of dynamic correlations (Kondo effect) [5].

A systematic approach to the Kondo effect is achieved by taking the single-particle mean-field spectrum of the LUMO (at each  $z$ ) as a starting point for a NRG simulation (see below for details). However, the DFT-LDA spectrum should not be used for this purpose since it lacks physical significance, being essentially an auxiliary quantity within a ground-state total-energy approach. A proper single-particle mean-field spectrum to be used as input to NRG must refer to electronic excitations (i.e., removal or addition of one electron) [6]. In particular, these excitations are subject to non-local correlation effects that are not included in DFT-LDA.

Mean-field spectra which take non-local correlation into account can be addressed within the standard  $GW$  approximation of MBPT [6]. In the present case, however, a full  $GW$  calculation is too demanding. We therefore employ a simplified, perturbative  $\text{LDA}+GdW$  approach which yields reliable QP energies  $E_n^{GdW} :=$

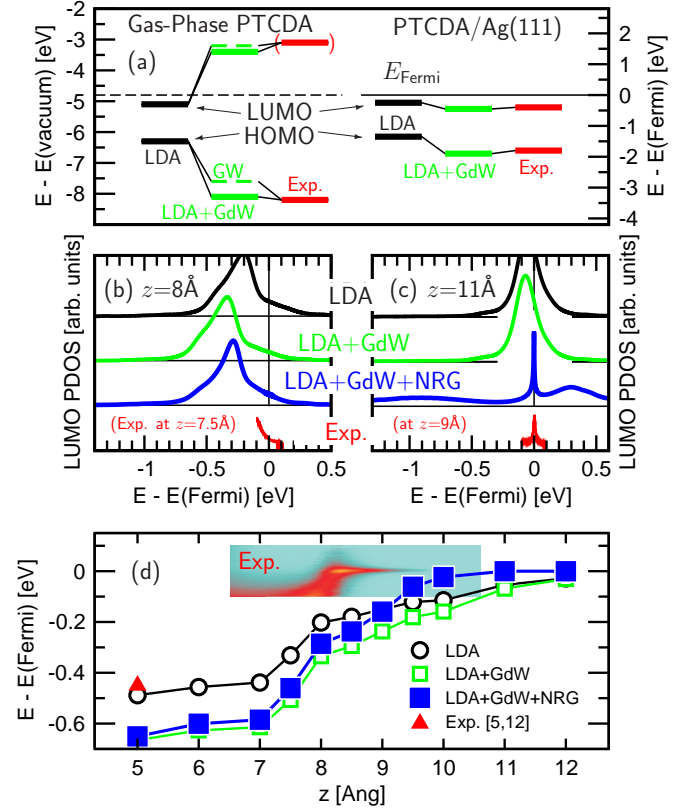


FIG. 2: (a) HOMO and LUMO energies of gas-phase PTCDA and PTCDA/Ag(111) (peak of the PDOS [16]; without STM tip). Experimental data are from Ref. [17, 18] (gas phase) and Ref. [11] (on Ag(111)). The two energy scales differ by  $E_F = E_{\text{vac}} - E_W$  ( $E_W =$  work function of Ag(111)). (b,c) LUMO spectra for the tip/PTCDA/Ag(111) junction [16] at tip heights of  $z = 8 \text{ \AA}$  and  $z = 11 \text{ \AA}$ . The experimental spectra are cuts through the  $dI/dV$  map of panel d, at  $z$ -values of  $7.5 \text{ \AA}$  and  $9 \text{ \AA}$ . (d) LUMO peak positions and experimental  $dI/dV$  color map, ranging from  $0 G_0$  (light blue) to  $0.10 G_0$  (yellow). Experiments were performed by approach-retraction cycles of the tip, with bias voltages increasing in steps of  $1 \text{ mV}$ .  $dI/dV$  was detected with a lock-in amplifier, modulation amplitude  $4 \text{ mV}$  and modulation frequency  $2.9 \text{ kHz}$ . For bias voltages exceeding  $\pm 100 \text{ meV}$  the tip-PTCDA contact becomes unstable. The experimental data point at  $-0.45 \text{ eV}$  is an estimate from Ref. 5 ( $-0.35 \text{ eV}$  with the tip attached to the PTCDA monolayer) and Ref. 12 (difference  $-0.1 \text{ eV}$  between single-molecule and monolayer spectra).

$E_n^{\text{LDA}} + \Delta_n^{\text{GdW}}$  on top of DFT-LDA from a QP Hamiltonian [21–23]

$$\hat{H}^{\text{QP,LDA}+GdW} := \hat{H}^{\text{LDA}} + iG(W - W_{\text{metal}}) \quad , \quad (1)$$

in which the QP self-energy correction  $\Delta^{\text{GdW}} := iG(W - W_{\text{metal}})$  results from the difference between the correctly screened Coulomb interaction ( $W$ ) and an interaction  $W_{\text{metal}}$  from hypothetical metallic screening (see Ref. [21] for details). The resulting QP corrections to DFT-LDA differ from standard  $GW$  QP corrections by less than 20

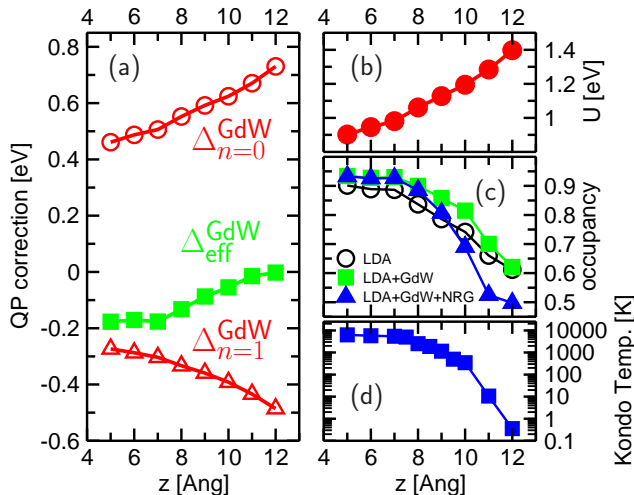


FIG. 3: Properties of the PTCDA LUMO at varying tip-surface distances  $z$ . (a) Mean-field QP correction (from LDA+ $GdW$ ) of the LUMO for various occupancies, i.e. (from top to bottom) for the state being empty, being partially occupied (at  $n_{\text{LDA}+GdW}$ ), and being filled. (b) Intra-state interaction  $U$  (from Eq. (2)). (c) Occupancy of the LUMO, resulting from LDA and LDA+ $GdW$ . Note that the number of electrons in the state is  $2 \cdot n$ . (d) Resulting Kondo temperature.

% [21–24]. For gas-phase PTCDA, LDA+ $GdW$  can easily be checked against a standard  $GW$  calculation and against the experiment. Fig. 2a shows that the  $GdW$  shifts ( $\Delta^{GdW} = -1.8$  eV for the HOMO and  $+1.7$  eV for the LUMO) agree well with standard  $GW$  results (both with our own and with those of Ref. [17]), in particular for the LUMO, and with experiment [17, 18], establishing LDA+ $GdW$  as a suitable method.

When the molecule is adsorbed on the surface, three features show up in  $\Delta^{GdW}$  and  $E^{GdW}$ : (i) Due to the metallic nature of the substrate, which screens the interaction inside the molecule non-locally [19–21], the  $GdW$  corrections are substantially reduced as compared to gas-phase PTCDA [25]. As shown in Fig. 3a, the QP corrections are below 0.5 eV for  $z = 5$  Å instead of almost 2 eV for the free molecule. Note, however, that as the molecule is removed from the metallic substrate, its screening becomes less metallic, and both  $W$  and  $\Delta^{GdW}$  grow again with increasing  $z$ . (ii) The  $GdW$  correction of the LUMO changes sign as a function of its occupation. If the state were empty (occupied) it would observe a  $GdW$  correction of  $\Delta_{n=0}^{GdW} > 0$  ( $\Delta_{n=1}^{GdW} < 0$ ), as shown in Fig. 3a. At partial occupation  $0 < n < 1$  (through charge transfer from the metal) we obtain an  $n$ -dependent QP shift  $\Delta^{GdW}(n) = (1-n)\Delta_{n=0}^{GdW} + n\Delta_{n=1}^{GdW}$ . (iii) Since the QP correction  $\Delta^{GdW}(n)$  shifts the whole LUMO spectrum  $f(E)$  rigidly with respect to the Fermi level, thereby changing its occupation by  $\Delta n$ , the classical (screened) Coulomb energy changes by  $2(\Delta n)U$  (the fac-

tor of 2 results from spin degeneracy), which must be added to  $\Delta^{GdW}$ , yielding an effective  $GdW$  correction of  $\Delta_{\text{eff}}^{GdW}(n) = (1-n)\Delta_{n=0}^{GdW} + n\Delta_{n=1}^{GdW} + 2(n-n_{\text{LDA}})U$ . Since the QP shift in turn determines  $n = \int_{-\infty}^{E_F} f^{GdW}(E) dE$  via  $f^{GdW}(E) = f^{\text{LDA}}(E - \Delta_{\text{eff}}^{GdW}(n))$ ,  $n$  and  $\Delta_{\text{eff}}^{GdW}$  must be determined self-consistently for each  $z$  (Fig. 3a,c). At small  $z$  we obtain a negative QP shift and a slight increase of  $n$  (as compared to  $n_{\text{LDA}}$ ) while at large  $z$  the QP shift approaches zero. A key ingredient into our calculations is the intra-state interaction energy  $U$ . It is given (for each  $z$ ) by

$$U = \int |\psi_{\text{LUMO}}(\mathbf{r})|^2 W(\mathbf{r}, \mathbf{r}') |\psi_{\text{LUMO}}(\mathbf{r}')|^2 d^3 r d^3 r' \quad (2)$$

Fig. 3b reveals that as a consequence of efficient metallic screening the  $U$  parameter is rather small (below 1 eV) for  $z < 8$  Å, but increases for larger  $z$ . For gas-phase PTCDA it amounts to 3.0 eV.

Results for the effective QP shift  $\Delta_{\text{eff}}^{GdW}$ , the  $U$  parameter, and the self-consistent occupation  $n$  are displayed in Fig. 3a-c. Although the QP correction turns out to be small, there is a clear trend from  $\Delta_{\text{eff}}^{GdW} = -0.17$  eV for  $z = 5$  Å to  $\Delta_{\text{eff}}^{GdW} \simeq 0$  eV for  $z = 12$  Å. This leads to an increased slope of the LDA+ $GdW$  QP peak position for  $z$  between 7 and 10 Å (Fig. 2d).

We finally extend our LDA+ $GdW$  calculation by including dynamical correlation in the NRG approach. Using the calculated values of  $U(z)$ , Eq. (2), we are able to extract the bare LUMO level positions  $\epsilon_0(z)$  and coupling functions  $\Gamma(E, z)$  from the LDA+ $GdW$  spectra at each  $z$ , by equating

$$f^{GdW}(E, z) \equiv \frac{1}{\pi} \Im \frac{1}{E - \epsilon_0(z) - nU(z) - \Gamma(E, z)}. \quad (3)$$

Together with  $U(z)$ , the so obtained  $\epsilon_0(z)$ ,  $\Gamma(E, z)$  enter the NRG calculation [7, 26] which yields the many-body LUMO spectra displayed in Fig. 2b-c [27].

The  $z$ -dependent renormalized peak position of the LDA+ $GdW$ +NRG data (full squares) can now be compared to the experimental data as shown in Fig. 2d. As in experiment, the calculation shows a fast-rising QP peak (slope 0.15 eV/Å for  $z$  between 8 and 10 Å), which also becomes pinned at  $E_F$  as soon as it reaches the Fermi energy (at  $z \approx 10$  Å). In both experiment and LDA+ $GdW$ +NRG, the pinned resonance is substantially sharper than the QP peak that moves up to  $E_F$  (see Fig. 2c). Since this sharpening to 14 meV (experiment at 9.7 Å) or 15 meV (theory at 11 Å) is neither observed in LDA nor in LDA+ $GdW$ , we can ascribe it to a dynamical correlation effect.

Note that for  $z \lesssim 8$  Å the LDA+ $GdW$  and LDA+ $GdW$ +NRG spectra are very similar (Fig. 2b). This is to be expected, since a nearly fully occupied state below  $E_F$  shows very weak dynamical correlation. In contrast, for  $z \gtrsim 9$  Å the difference between LDA+ $GdW$

and LDA+*GdW*+NRG becomes dramatic. While LDA+*GdW* still yields a single LUMO peak (Fig. 2c), the LDA+*GdW*+NRG spectrum shows a three-peak structure, with two single-particle side bands (at  $-0.9$  eV and  $+0.3$  eV for  $z=11$  Å, separated by  $\sim U$ ) and a Kondo resonance at  $E_F$  (Fig. 2c). The Kondo resonance is also observed in experiment (bottom of Fig. 2c and sharp horizontal line in Fig. 2d).

In Fig. 3d the evolution of the Kondo temperature  $T_K(z)$  is plotted.  $T_K$  has been determined from the NRG calculation as the temperature at which 40 % of the local moment in the LUMO is screened (Wilson criterion). For  $z < 9$  Å  $T_K$  is a few thousand K, because in this  $z$ -range  $U$  and  $\Gamma$  are of similar size, and hence there is no clear separation between spin and charge fluctuation energy scales. In other words, in this regime  $T_K$  is equivalent to the charge fluctuation scale  $\Gamma$ . Physically, this means that screening of the small residual moment that is left by the total occupancy of 1.8 electrons in the LUMO is accomplished by uncorrelated charge fluctuations in and out of the level. At  $z = 12$  Å  $T_K$  has dropped to  $T_K < 1$  K, caused by the increase of the ratio  $U/\Gamma$  which leads to the clear separation of spin and charge energy scales. Accordingly,  $T_K$  is now a Kondo temperature in the proper sense, related to the energy scale of correlated screening of a fixed moment in the LUMO by virtual spin fluctuations. In experiment, the Kondo resonance can only be followed up to  $z \approx 10$  Å because of decreasing signal strength, but at  $9.7$  Å the Kondo resonance has a FWHM of 14 meV, in good agreement with a predicted Kondo temperature of the order 100 K (Fig. 3d).

One remaining difference between our LDA+*GdW*+NRG data and experiment is the  $z$ -position at which the QP peak reaches  $E_F$  and turns into the resonance. This could be due to the underestimation of the Ag(111) work function within the underlying DFT-LDA ( $\sim 4.6$  eV instead of the experimental value of 4.8 eV), which persists throughout our calculations. Taking this into account, the Fermi level in all theoretical spectra should be lowered by 0.2 eV, i.e. all molecular QP features in Fig. 2 would be at higher energies by 0.2 eV. The LDA+*GdW*+NRG peak would then reach the Fermi level at about  $z \approx 8$  Å.

In conclusion, we have presented an approach to calculating electronic spectra that systematically includes non-local and dynamic correlation effects. It correctly predicts the mechanical gating of the tip/PTCDA/Ag(111) junction. Because of its computational efficiency, this state-of-the-art approach to electronic spectra should be widely applicable.

We thank the Deutsche Forschungsgemeinschaft for financial support (Grants RO 1318/6-1, AN 275/6-2 and TA 244/5-2).

- 
- \* Electronic address: Michael.Rohlfing@uos.de
- [1] L. Lafferentz et al., *Science* **323**, 1193 (2009).
  - [2] I. Fernandez-Torrente, K.J. Franke, and J.I. Pascual, *Phys. Rev. Lett.* **101**, 217293 (2008).
  - [3] Y. Wang et al., *J. Am. Chem. Soc.* **131**, 3639 (2009).
  - [4] Y.F. Wang et al., *Phys. Rev. Lett.* **104**, 176802 (2010).
  - [5] R. Temirov et al., *Nanotechnology* **19**, 065401 (2008).
  - [6] G. Onida, L. Reining, and A. Rubio, *Rev. Mod. Phys.* **74**, 601 (2002).
  - [7] R. Bulla, T. A. Costi, and T. Pruschke, *Rev. Mod. Phys.* **80**, 395 (2008).
  - [8] Previous studies of PTCDA/Ag(111) showed that DFT employing the LDA yields reliable structural data in good agreement with available experiments [9, 11] and with more elaborate many-body total-energy approaches [13], although many details of long-range correlation are missing from the DFT-LDA. We thus employ DFT-LDA throughout this work.
  - [9] A. Hauschild et al., *Phys. Rev. Lett.* **94**, 036106 (2005); *Phys. Rev. Lett.* **95**, 209602 (2005).
  - [10] S.X. Du et al., *Phys. Rev. Lett.* **97**, 156105 (2006).
  - [11] A. Kraft et al., *Phys. Rev. B* **74**, 041402 (2006).
  - [12] L. Kilian et al., *Phys. Rev. Lett.* **100**, 136103 (2008).
  - [13] M. Rohlfing and T. Bredow, *Phys. Rev. Lett.* **101**, 266106 (2008).
  - [14] M. Rohlfing, R. Temirov, and F. S. Tautz, *Phys. Rev. B* **76**, 115421 (2007).
  - [15] Choosing Ag as tip material is motivated by the experimental tip preparation method, in which a tungsten tip is dipped into the Ag substrate, picking up some silver material. Tungsten as tip material leads to equivalent results as discussed here (apart from somewhat stronger tip-molecule bond energy for tungsten).
  - [16] The LDA spectrum of the LUMO in contact with the substrate results from projection of all states of the respective system ( $|\psi_n\rangle$ ) onto  $|\psi_{\text{LUMO}}\rangle$ , i.e.  $f_{\text{LDA}}(E) = \sum_n |\langle \psi_n | \psi_{\text{LUMO}} \rangle|^2 \delta(E - E_n^{\text{LDA}})$  (projected density of states, PDOS). The occupancy of the state is  $n = \int_{-\infty}^{E_F} f(E) dE$ .
  - [17] N. Dori et al., *Phys. Rev. B* **73**, 195208 (2006).
  - [18] We are not aware of a direct measurement of the electron affinity (EA) of gas-phase PTCDA. The EA of bulk PTCDA was reported as 4.4 eV by Xue and Forrest, *Phys. Rev. B* **69**, 245322 (2004) and as 4.12 eV by Kampen et al., *J. Phys. Chem. C* **15**, S2679 (2003). If one assumes (similar to the ionization potential) a bulk-screening effect of 1.2 eV, an EA between 2.88 eV and 3.2 eV would result for gas-phase PTCDA.
  - [19] J.B. Neaton, M.S. Hybertsen, and S.G. Louie, *Phys. Rev. Lett.* **97**, 216405 (2006).
  - [20] K.S. Thygesen and A. Rubio, *Phys. Rev. Lett.* **102**, 046802 (2009).
  - [21] M. Rohlfing, <http://arxiv.org/abs/1008.3492> (cond-mat)
  - [22] F. Gygi and A. Baldereschi, *Phys. Rev. Lett.* **62**, 2160 (1989).
  - [23] V. Fiorentini and A. Baldereschi, *Phys. Rev. B* **51**, 17196 (1995).
  - [24] C.S. Wang and W.E. Pickett, *Phys. Rev. Lett.* **51**, 597 (1983).
  - [25] For PTCDA on Ag(111), our LDA+*GdW* method in-

volves a further approximation, i.e. the evaluation of  $G$  from molecular states only (i.e. from a calculation without substrate and tip), disregarding the hybridisation with substrate states. This is justified by the fact that the molecular states are only slightly shifted and broadened due to contact with the substrate.

[26] R. Peters, T. Pruschke, and F. B. Anders, Phys. Rev. B

**74**, 245114 (2006).

[27] Since the LDA calculation indicates a weak influence of the tip onto the spectra, we also neglect the voltage dependence of the spectral function which would be only significant for a symmetric junction [5, 28].

[28] F. B. Anders, Phys. Rev. Lett. **101**, 066804 (2008)